Evaluation of a Variable Facesheet Liner Configuration in Grazing Incidence for Broadband Noise Reduction

M. C. Brown* and M. G. Jones†
NASA Langley Research Center, Hampton, VA 23681

Tests were conducted in the NASA Langley Grazing Flow Impedance Tube (GFIT) to determine the broadband noise reduction capability of a variable facesheet liner. Three uniform liners were designed to achieve sound absorption over distinct frequency regimes at Mach 0.0. Each liner was fabricated and tested in the GFIT at sound pressure levels of 120 and 140 dB, and at tangential flow velocities up to Mach 0.5. A variable facesheet liner was fabricated to combine the geometries of these three liners, such that the facesheet geometry (hole diameter and porosity) was varied across the liner surface. The Prony method was used to educe the impedance of each sample, and these impedances were input to the CHE (Convected Helmholtz Equation) propagation code to predict the acoustic pressure profiles in the GFIT. Comparisons of predicted and measured acoustic pressure profiles were used to confirm the uniformity of all four liners, and to demonstrate the suitability of the CHE code in the analysis of the variable facesheet concept. Results showed good comparison at no flow and at Mach 0.3, and acceptable comparison at Mach 0.5. The variable facesheet liner provided enhanced broadband noise reduction at the no-flow condition for which it was designed, but further optimization is needed to target flow conditions.

I. Introduction

This investigation is a continuation of a previous study evaluating the acoustic benefits of a variable facesheet liner for broadband noise reduction.[1] The objective of the study is to explore the possibility of achieving broadband sound absorption, by varying the facesheet porosity and hole diameter for each core chamber, while keeping the facesheet thickness and core depth constant. In the previous investigation, test sample candidates were selected using an impedance prediction model[2,3] developed at the NASA Langley Research Center, and evaluated at no flow and 120 dB. Four samples were fabricated and tested in the Normal Incidence Tube (NIT): three uniform facesheets and one nonuniform (or variable) facesheet. Impedances educed from the NIT results were used as inputs in the Convected Helmholtz Equation (CHE) propagation code[4] developed at NASA Langley to synthesize the acoustic pressure field in the Grazing Flow Impedance Tube (GFIT). Initial results showed that for a no flow condition, there is a possibility to significantly extend the frequency range of absorption for a single-layer liner by manipulating the facesheet characteristics. Conventional single-layer acoustic liners, which consist of a perforated uniform facesheet over a honeycomb core, are commonly used to reduce fan noise emitted from aircraft engine nacelles. Although initial results showed that a variable facesheet liner exhibited better attenuation over a wider range of frequencies in comparison with a traditional uniform facesheet liner for no flow, further investigation was needed to assess acoustic performance in a grazing incidence waveguide, with and without flow. Variable facesheet liners provide a different approach to achieve broadband acoustic benefits, while minimizing manufacturing complexities, and without sacrificing weight. Each of the four liner configurations was fabricated to 2" by 18" (active area) sizes and tested in the GFIT with (Mach 0.3 and 0.5) and without flow at two sound pressure levels of 120 and 140 dB.

*Research Engineer, Research Directorate, Aeroacoustics Branch, martha.c.brown@nasa.gov.
†Senior Research Scientist, Research Directorate, Structural Acoustics Branch, michael.g.jones@nasa.gov, AIAA Associate Fellow.

II. Experimental Methods

A. Evaluation Liners

In the previous investigation, three uniform configurations (N01, N02, and N03) and a variable facesheet configuration (N04) were fabricated and tested in the NIT. Figure 1 outlines the characteristics of each sample for the reader's reference. The hole diameter is represented by d, in inches. Porosity, σ is determined by calculating the total area of the perforate holes in a core chamber divided by the total surface area of that respective core chamber. In these samples, the dimensions of each core chamber are 0.3" by 0.3" square. The NIT samples contain a grid of 5 by 5 core chambers for a 2" by 2" sample size. The thickness of the facesheets, t, is fixed at 0.030". Corresponding GFIT samples were constructed using similar designs, as shown in Fig. 2 and described in Table 1. Note that for the distributed liner (G04), the N04 2" by 2" sample is replicated nine times (totaling 18" active liner length). The depth of the core for all the samples is 1.500". The liners used in this study are composite structures consisting of a perforated facesheet, a square-shaped core, and a rigid back plate. The reader should note that a square-shaped core, was fabricated instead of the traditional honeycomb-shaped core to facilitate simpler modeling. These GFIT samples were fabricated with the intent of investigating the effects of a variable facesheet liner with and without flow.

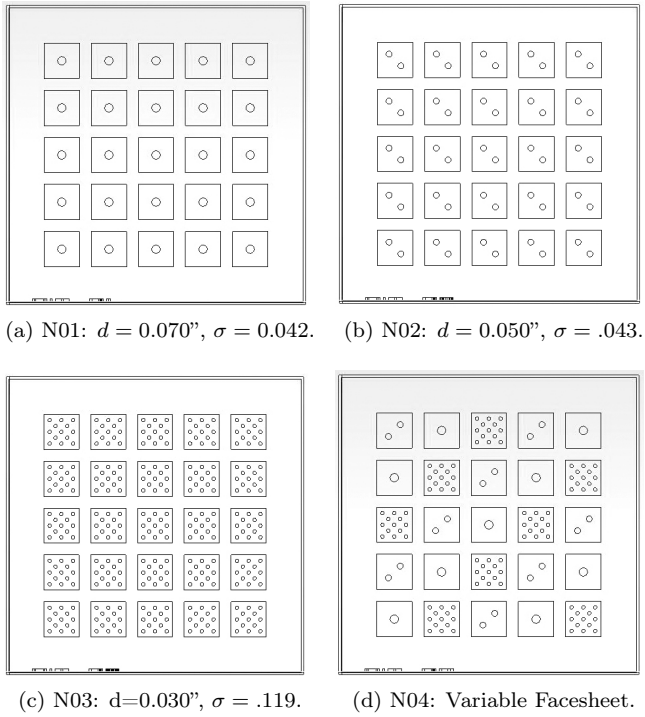

(a) N01: $d = 0.070$", $\sigma = 0.042$.

(b) N02: $d = 0.050$", $\sigma = .043$.

(c) N03: d=0.030", $\sigma = .119$.

(d) N04: Variable Facesheet.

Figure 1: Sketch of NIT samples.

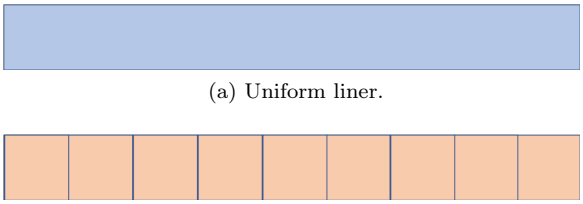

(a) Uniform liner.

(b) Distributed-facesheet liner.

Figure 2: Sketch of GFIT samples.

Table 1: GFIT samples, 18” active length.

Nomenclature	Description
G01	Uniform Liner: $d = 0.070”, t = 0.030”, \sigma = 0.042$
G02	Uniform Liner: $d = 0.050”, t = 0.030”, \sigma = 0.043$
G03	Uniform Liner: $d = 0.030”, t = 0.030”, \sigma = 0.119$
G04	Variable facesheet Liner: N04 (2”) replicated nine times

B. Grazing Flow Impedance Tube (GFIT)

The Grazing Flow Impedance Tube (GFIT, see Fig. 3) is used to evaluate the acoustic performance of each liner. The GFIT has a cross-sectional geometry of 2” wide by 2.5” high, such that higher-order modes in the horizontal and vertical dimensions cut-on at different frequencies. It allows evaluation of acoustic liners with lengths from 2” to 24”. The surface of the test liner forms a portion (18” active length for this investigation) of the upper wall of the flow duct. For this investigation, the source section consists of twelve acoustic drivers mounted upstream (exhaust mode) of the test section. These drivers are used to generate tones (one frequency at a time) at source sound pressure levels (SPL) of 120 and 140 dB over a frequency range of 400 Hz to 3000 Hz, in increments of 100 Hz. These tests were conducted at flow speeds of Mach 0.0, 0.3, and 0.5.

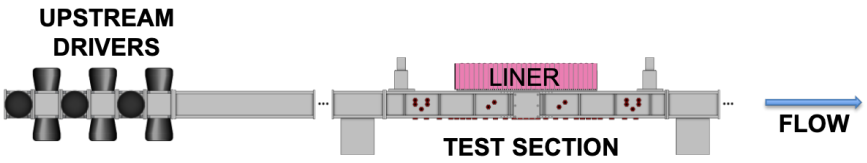

Figure 3: Artist rendition of Grazing Flow Impedance Tube (GFIT).

Fifty-three flush-mounted microphones located in the lower wall (opposite the liner) are used to measure the acoustic pressure field over the axial length of 40” (see Fig. 4). Note the leading edge of the liner is 8.2” from the x=0” plane. A cross-spectrum signal extraction method[5] is used to determine the amplitudes and phases at each of the microphone locations relative to the amplitude and phase at the reference microphone location.

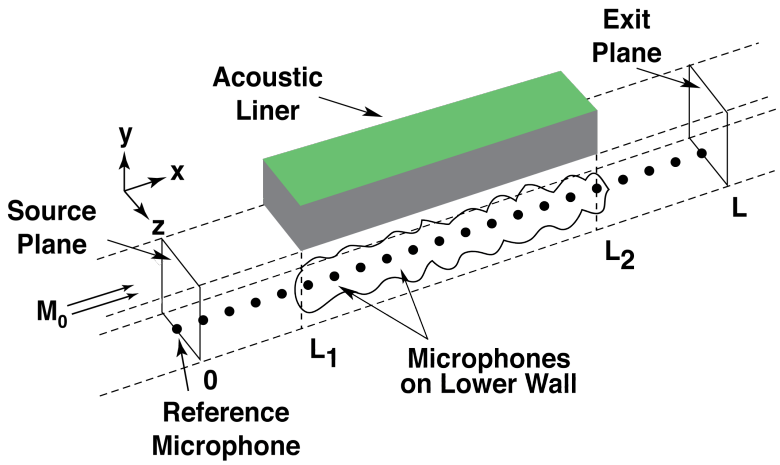

Figure 4: Sketch of Grazing Flow Impedance Tube (GFIT) test section.

III. Acoustic Performance

A. Impedance Eduction Methodology

The Prony impedance eduction method[6] solves a linear system of equations formed from the complex acoustic pressures measured with the microphones located on the wall opposite the liner. The coefficients derived are used to create a polynomial equation, and the complex roots of that polynomial are used to educe the impedance of a liner. The liner is assumed to be uniform and locally-reacting, and the mean flow is assumed to be uniform for this method. Clearly, the G01, G02, and G03 liners satisfy this requirement of uniformity, but the G04 liner is comprised of a distribution of three distinct facesheet geometries, i.e., it is a variable facesheet. However, previous studies[7] demonstrated that distributed impedances could be treated as a uniform, *smeared* impedance if the variability is confined to within one-third of a wavelength at the highest frequency of interest. In this study, the highest frequency of interest is 3.0 kHz, and $\lambda/3$ ~ 1.500". Since the variability in the G04 liner is confined to a much smaller spatial extent than 1.500", this liner is also assumed to provide a uniform acoustic impedance.

B. Acoustic Propagation Comparison

The CHE acoustic propagation code is used to predict the effects of the respective liners on sound propagation through the GFIT. These predictions are compared against acoustic pressures measured via the microphones on the wall opposite the liner in the GFIT.

The CHE propagation code requires a number of inputs. First, the average Mach number, static temperature, and static pressure are taken from the measured data acquired in the GFIT. The acoustic pressures (SPL and phase) at the leading and trailing edges of the computational domain (x=0 and x=L in Fig. 4) are also taken from the measured data. The final input is the impedance educed using the Prony method.

Comparison of predicted and measured acoustic pressure axial profiles are presented in the Results section. These comparisons are used to assess the validity of the assumption that the variable facesheet liner presents a uniform impedance at its surface. If this is demonstrated to be correct, it suggests the process used to design an optimal variable facesheet liner is also valid.

IV. Results

Figures 5 and 6 present comparisons of acoustic impedance spectra educed from acoustic pressure data acquired in the NIT and GFIT with source sound pressure levels (SPLs) of 120 and 140 dB, respectively. All impedances presented in this paper are normalized by ρc, where ρ and c represent the density and

sound speed of air at ambient conditions. The normalized resistance (indicated by "RES' in the legend) and normalized reactance (indicated by 'REA' in the legend) are plotted on the same graph.

The acoustic pressure impinges directly (normal incidence) onto the surface of the liner in the NIT but propagates over the GFIT liner at grazing incidence. However, the impedance educed from the acoustic pressures measured on the wall opposite the liner in the GFIT using the Prony method is also a normal incidence impedance. Thus, the impedance for a liner mounted in the NIT should be similar to that educed for a similarly constructed liner in the GFIT when the GFIT is operated without mean flow.

Figure 5 presents results based on data acquired with a 120 dB source. For the NIT, this means that the surface of the liner is exposed to 120 dB sound over the entirety of its surface. For the GFIT, however, only the leading edge of the liner is exposed to this level. For data acquired at frequencies where the liner provides sound attenuation, the sound pressure level (SPL) decreases along the length of the liner. This change in SPL has no impact on the impedance of a linear liner, but it can have a noticeable effect for nonlinear liners.

Since perforate liners are known to be weakly nonlinear, this is expected to cause some differences between the impedance spectra educed with the NIT and GFIT (at Mach 0.0). Despite these differences, the impedance spectra compare favorably for a source SPL of 120 dB (Fig. 5). It should be noted that spurious impedances were observed for frequencies below 500 Hz and above 2800 Hz, so those frequencies are not included in the presented results.

For the two lower porosity liners (Figs. 5a and 5b), the NIT and GFIT impedance spectra are observed to diverge slightly at the higher frequencies. Also, the impedance for the G02 liner near 2250 Hz is clearly anomalous, as the educed resistance is negative. Other than a slight disparity at the lowest frequencies, the impedances educed for the higher porosity liners (N03 and G03, Fig. 5c) compare extremely well. Finally, the impedances educed with the variable facesheet liners (N04 and G04, Fig. 5d) compare favorably away from the antiresonance that occurs near 1500 Hz, but diverge near that frequency. An antiresonance for a single-layer liner causes the resistance to experience a noticeable increase and the reactance to transition from positive to negative over a relatively short frequency range. Perhaps more importantly, limited sound absorption in this frequency range causes increased difficulty in the impedance eduction process, thereby introducing more uncertainty into the results.

It should be noted that the resistances for the three uniform liners are quite small. The reactance for a uniform perforate liner consists of a cavity reactance and a mass reactance. The cavity reactance follows the expected $-cot(kD)$ pattern, where k is the freespace wavenumber and D is the core depth (in inches), and should therefore be the same for each of these liners (constant depth of 1.500"). The mass reactance (related to the mass of the air that is traveling through the perforate) is a linear function of frequency, and increases with increasing hole diameter, increasing sheet thickness, or decreasing porosity.[8] This suggests the mass reactance should be larger for the G01 and G02 liners than for the G03 liner. This combination of cavity and mass reactance causes the frequency where resonance occurs to increase with decreasing mass reactance, as is shown in the educed impedances. The educed resonance occurs near 1250 Hz for both the G01 and G02 liners, but increases to about 1950 Hz for the G03 liner.

This disparity in resonance frequencies is the key to the design of the N04 and G04 variable facesheet liners. When the three distinct geometries are combined into a single liner, the resultant liner provides increased resistance over an extended frequency range and provides two distinct resonances near 1100 Hz and 1700 Hz. This causes the variable facesheet liner to provide increased attenuation over a wider frequency range than is achieved with any of the three uniform liners.

Figure 6 presents the corresponding results for data acquired with a 140 dB source. An increase in the source SPL causes the resistance of the liner to increase, as is evident in the educed results. The comparison between the NIT and GFIT results remains favorable for the N03 configuration, but degrades somewhat for the N01 and N02 configurations, especially at the higher frequencies. The resistances educed for the GFIT liners tend to be independent of frequency, whereas those educed for the NIT liners show increases at frequencies at or just below resonance. The reactances for the N03 and G03 liners compare quite well, but those for the other two configurations diverge more noticeably than for the 120 dB case, especially at the higher frequencies. This is believed to be at least partially due to the nonlinearity of the uniform liners, especially those with very low open area ratios. As the sound is absorbed by the GFIT liner, the SPL decreases from 140 dB at the liner leading edge to a lower value (depends on the frequency). Thus, the impedance that is educed under the uniform impedance assumption is closer to that observed for the lower SPL, whereas the entire surface of the NIT sample is exposed to a constant level (140 dB in this case).

Regardless, the impedance of the variable facesheet liner (G04) appears to be dominated by the effects observed for the G01 and G02 liners.

Also observe that the N04 variable facesheet liner exhibits only one resonance (see Fig. 6d). As the SPL increases, the resistance increases due to the low porosity chambers becomes sufficiently large to cause the two resonances to merge into one. Interestingly, the two resonances remain in the GFIT results for the G04 liner. As noted above, attenuation over the length of the G04 liner causes much of the liner to experience lower SPLs, such that this increase in resistance for the low porosity chambers is not as significant. This merging of resonances is not observed in the GFIT results for this condition. As a result, the G04 liner is expected to provide good attenuation over a smaller frequency bandwidth at this condition. This is not entirely unexpected, as this variable facesheet configuration was initially designed for the Mach 0.0, 120 dB test condition.

Figure 7 presents the impedance spectra educed for the G04 liner from data acquired in the GFIT at a source SPL of 120 dB, for Mach 0.3 and 0.5 flow conditions. At Mach 0.3 (Fig. 7a), the impedance is closer to that observed for the Mach 0.0, 140 dB case than for the Mach 0.0, 120 dB case, but the resistance is slightly higher and the slope of the reactance spectrum is significantly lower. As the flow is increased to Mach 0.5 (Fig. 7b), the resistance increases, and the reactance slope becomes even lower. Anomalous behavior is also evident at the lower frequencies (the impedance for this liner is expected to be a smooth function of frequency).

As the source SPL is increased to 140 dB (Fig. 8), the impedance spectra become smoother, suggesting the impedance eduction process may be improved for data acquired at this level. This seems reasonable, as the signal-to-noise ratio is higher for the 140 dB case.

Perhaps more importantly, the resistance spectra for both source SPLs and flow Mach numbers are well above the optimum values (which depend on the frequency and the flow Mach number, but remain below unity) and the reactance spectra are quite similar to that expected for a single-layer liner, i.e., the reactance spectra at both flow conditions provide a single resonance in the frequency range of interest. As a result, the 140 dB cases at both Mach 0.3 and 0.5 are not expected to provide significant broadband absorption.

Figure 9 presents the attenuation over the length of a GFIT liner sample for the Mach 0.0 condition at 120 and 140 dB, respectively. Attenuation is determined by subtracting the acoustic pressure at the trailing edge from the acoustic pressure at the leading edge of a liner–the higher the attenuation, the more absorption at a particular frequency. For the uniform liners (G01, G02, and G03), there is one peak at their respective resonant frequencies as shown in Figs. 5a, 5b, and 5c. For the variable facesheet liner (G04), there are two peaks, which correspond to their resonant frequencies from Fig. 5d. Although the uniform liners outperformed the variable facesheet liner at some frequencies, the variable facesheet liner absorbed well over a wider range of frequencies (greater than 10 dB of attenuation from 1000 to 1900 Hz).

Figures 10a and 10b present the attenuation at 120 dB for Mach 0.3 and 0.5, respectively. The results at the 140 dB are very close to the results obtained at the 120 dB condition, therefore, those results are not presented in this paper. For the flow cases, G03 outperforms the G04 liner between 1100 and 2500 Hz. Outside of this frequency range, the results are not differentiable. The reader should note that although the liner was optimized for flow, it did perform well in attenuating sound over a range of frequencies. The authors are encouraged that if a variable facesheet liner were optimized for flow, the acoustic performance will be improved.

As was shown in the earlier study,[1] the variable facesheet liner (G04) provides good attenuation over an increased frequency bandwidth relative to that achieved with each of the three uniform liners when there is no mean flow and the source level is 120 dB. However, when the source level is increased or the mean flow is engaged, the variable facesheet liner no longer outperforms the uniform liners. Instead, the bandwidth of peak attenuation is higher for the G03 liner than for the G04 liner. This result is believed to be due to the change from two distinct resonances to one as either the source level or Mach number is increased. However, this does not mean that the variable facesheet concept is confined to applications of low SPL and no flow. Instead, it suggests that the design process needs to consider the higher source SPL and Mach numbers. This is intended to be the focus of the next phase of this study.

In order to complete this variable facesheet concept (G04), it is important to demonstrate the validity of the computational tools used in the design. A key component in this task is to demonstrate that the CHE propagation code is appropriate for the evaluation of variable facesheet liners. Figures 11-13 present comparisons of predicted and measured SPL profiles for the case where the G04 liner is mounted in the

GFIT. Figure 11 presents results for the Mach 0.0 condition, and for test frequencies of 1.0, 1.5, and 2.0 kHz. The comparison is good over the axial extent of the liner (from x=8" to x=26"). It deteriorates slightly over the downstream portion of the duct, but the comparison remains acceptable. The largest attenuation of 15 to 20 dB occurs at 1.0 kHz.

For the Mach 0.3 condition (Fig. 12), the comparisons are excellent for the lower two frequencies, and remain acceptable for the highest frequency. Interestingly, the peak attenuation (of these three arbitrarily chosen frequencies) occurs at 2.0 kHz. Clearly, the changes in impedance noted earlier have a direct effect on the resultant attenuation. More importantly, the favorable comparison between predicted and measured SPL profiles (and the corresponding phase profiles, not shown here for the sake of brevity) indicates that the CHE propagation code can be confidently used in the design process. For the Mach 0.5 condition (Fig. 13), the comparisons show similar trends (less attenuation than for the Mach 0.0 case), and the prediction is unable to accurately predict the standing wave pattern downstream of the trailing edge of the liner.

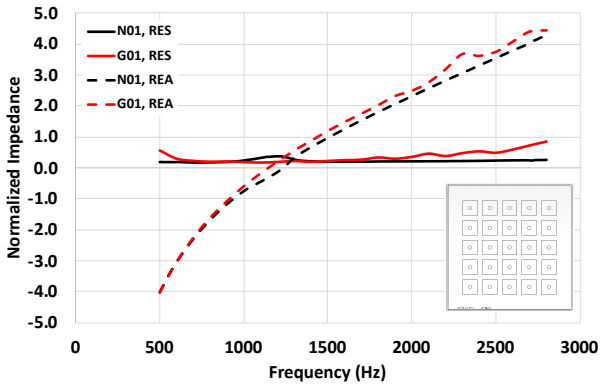

(a) N01 vs. G01, $\sigma = 0.042$.

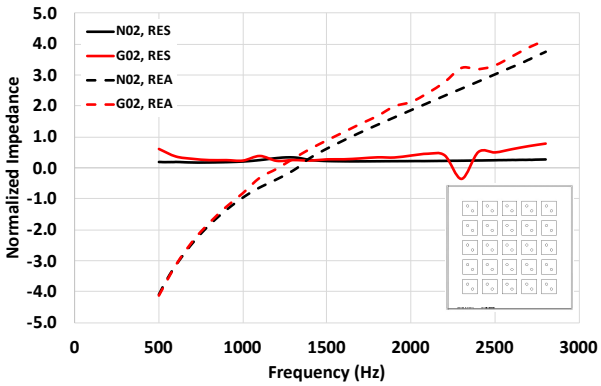

(b) N02 vs. G02, $\sigma = 0.043$.

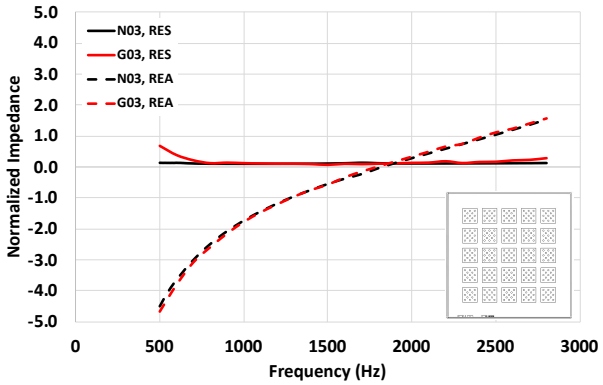

(c) N03 vs. G03, $\sigma = 0.119$.

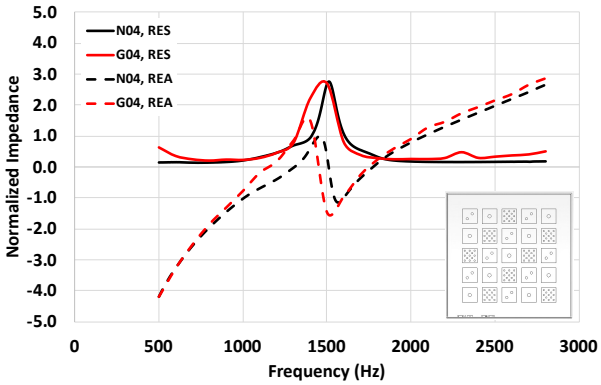

(d) N04 vs. G04.

Figure 5: Normalized impedance for NIT and GFIT liner samples, Mach 0.0, 120 dB.

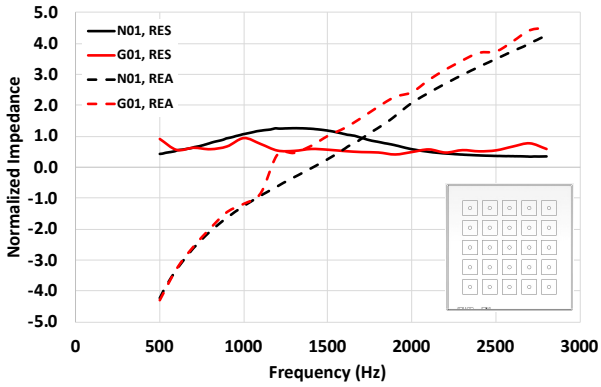

(a) N01 vs. G01, $\sigma = 0.042$.

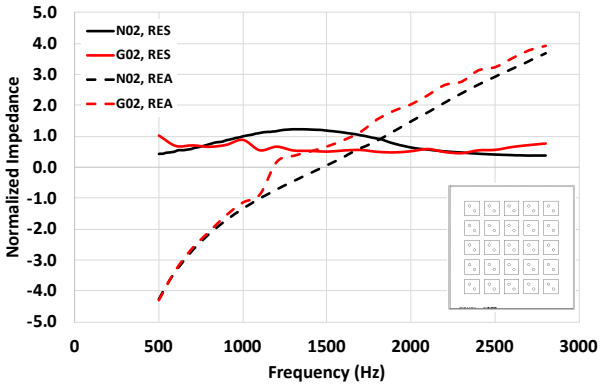

(b) N02 vs. G02, $\sigma = 0.043$.

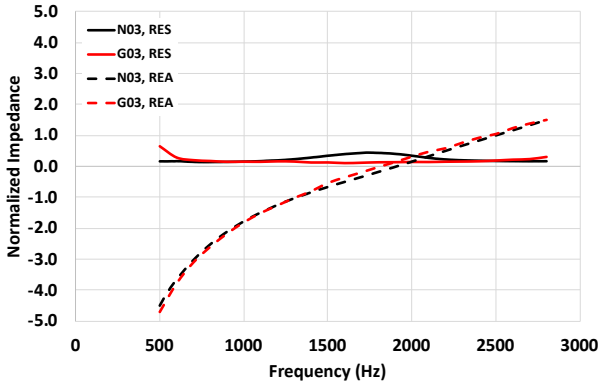

(c) N03 vs. G03, $\sigma = 0.119$.

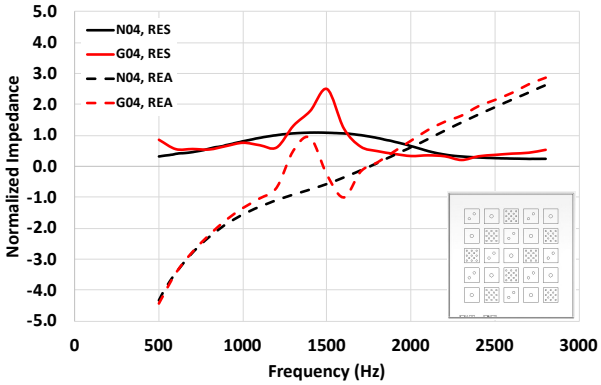

(d) N04 vs. G04.

Figure 6: Normalized impedance for NIT and GFIT liner samples, Mach 0.0, 140 dB.

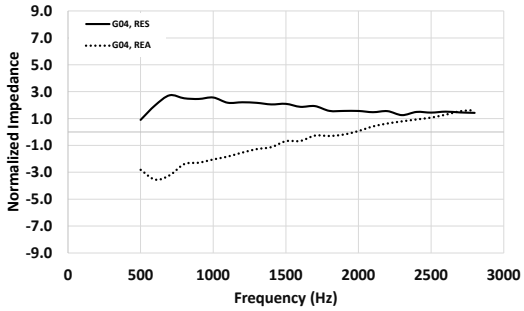

(a) Mach 0.3.

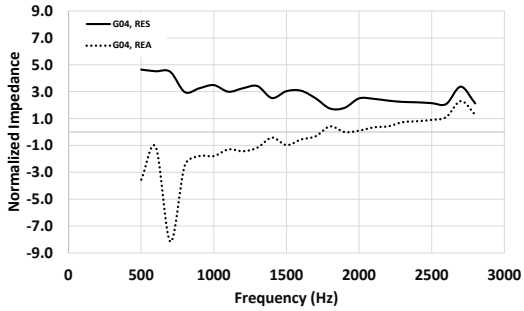

(b) Mach 0.5.

Figure 7: Normalized impedance for variable facesheet liner sample (G04), 120 dB.

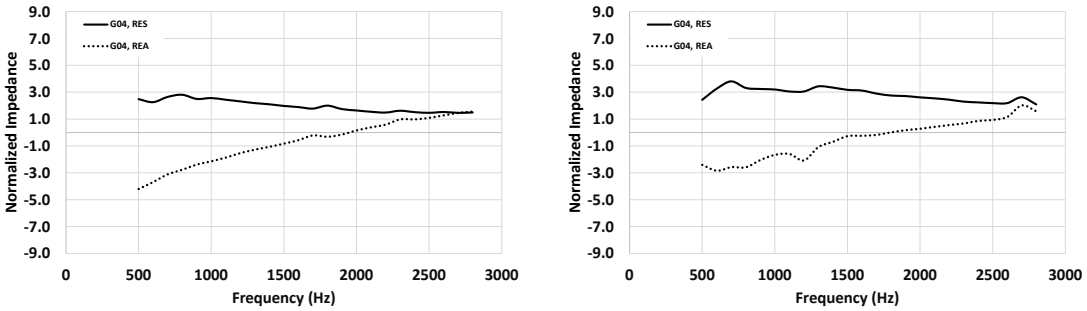

(a) Mach 0.3. (b) Mach 0.5.

Figure 8: Normalized impedance for variable facesheet liner sample (G04), 140 dB.

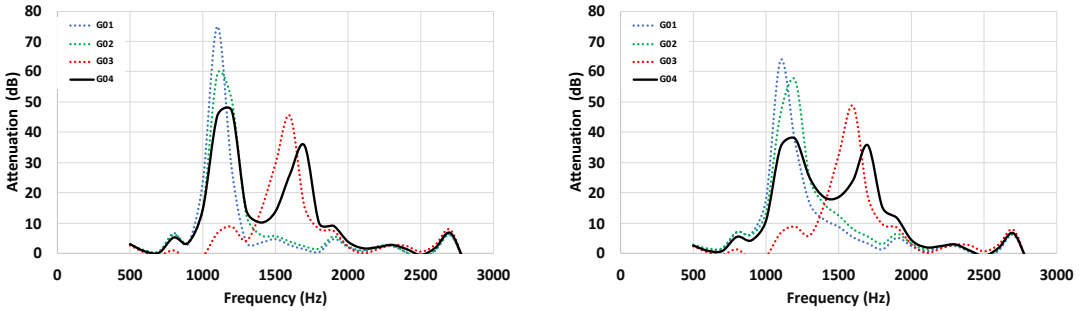

(a) 120 dB. (b) 140 dB.

Figure 9: Attenuation over length of GFIT liner at 120 and 140 dB, Mach 0.0.

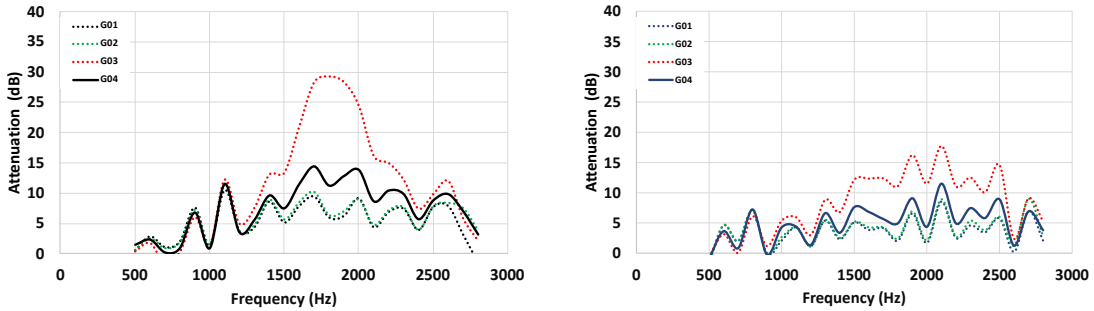

(a) Mach 0.3. (b) Mach 0.5.

Figure 10: Attenuation over length of GFIT liner at 120 dB with flow.

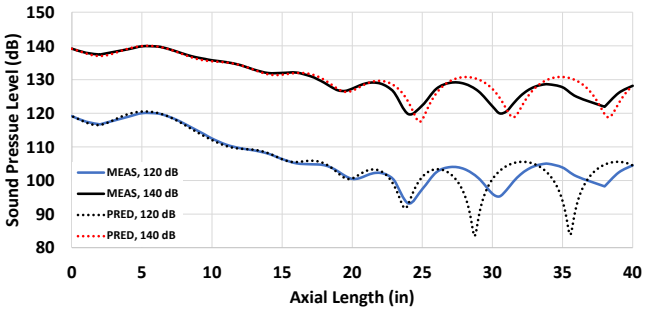

(a) 1000 Hz.

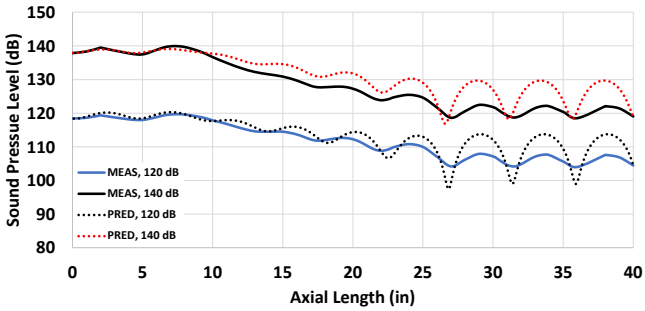

(b) 1500 Hz.

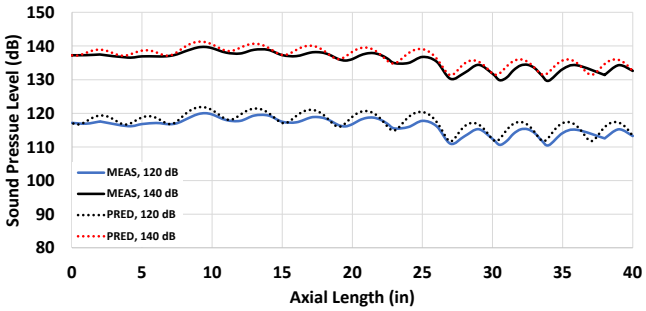

(c) 2000 Hz.

Figure 11: Comparison of measured and predicted acoustic pressures along the axial length of GFIT at 120 and 140 dB, Mach 0.0.

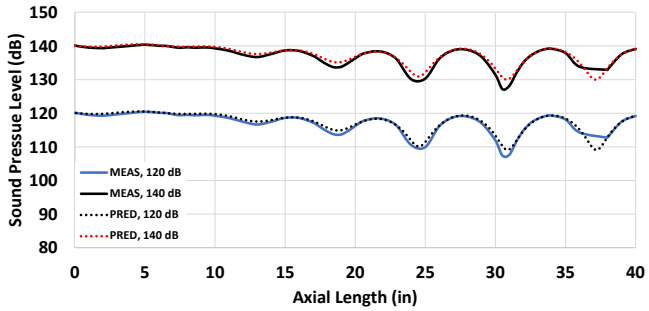

(a) 1000 Hz.

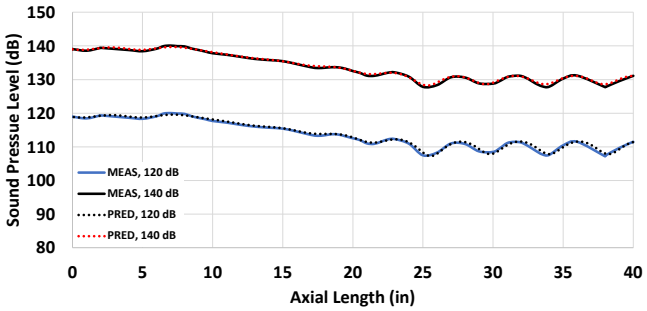

(b) 1500 Hz.

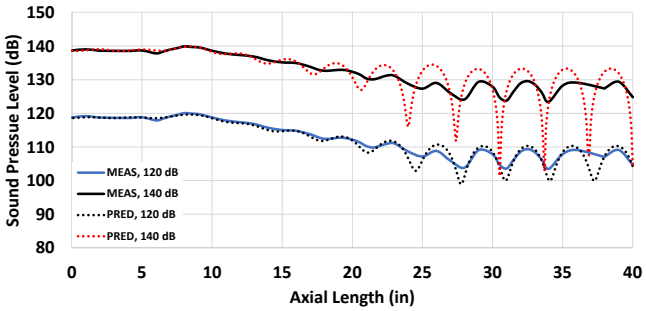

(c) 2000 Hz.

Figure 12: Comparison of measured and predicted acoustic pressures along the axial length of GFIT at 120 and 140 dB, Mach 0.3.

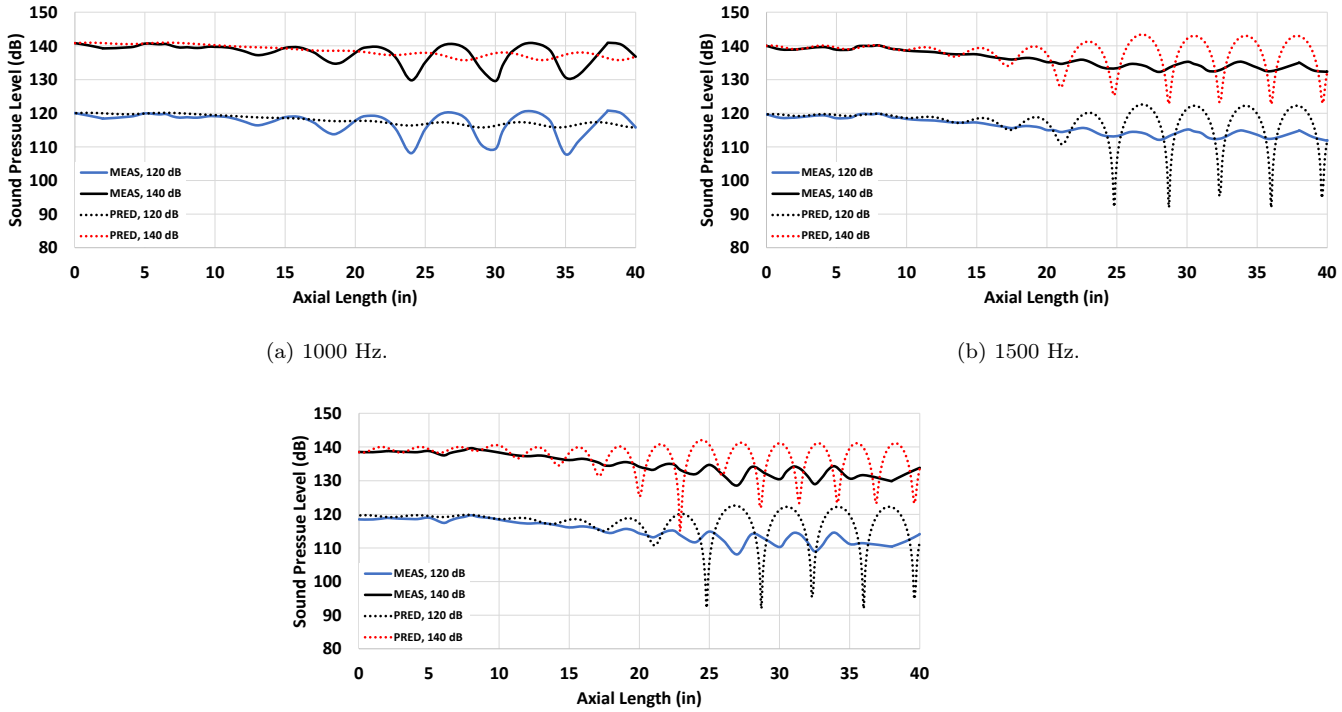

(a) 1000 Hz.

(b) 1500 Hz.

(c) 2000 Hz.

Figure 13: Comparison of measured and predicted acoustic pressures along the axial length of GFIT at 120 and 140 dB, Mach 0.5.

V. Concluding Remarks

This paper is a continuation of a previous study that evaluated the acoustic benefits of a variable facesheet liner for broadband noise reduction. A variable facesheet liner was fabricated to combine the geometries of three uniform facesheet liners, such that the facesheet geometry (hole diameter and porosity) was varied across the liner surface to achieve the best possible broadband attenuation at 120 dB and no flow. A disparity in resonance frequencies was key to the design of the variable facesheet liner, for which two distinct resonance frequencies were observed within the frequency range of interest. This caused the variable facesheet liner to provide increased attenuation over a wider frequency range than was achieved with any of the three uniform liners.

The previous study focused on smaller configurations that were tested in the NIT. In this investigation, larger versions of the NIT samples were tested in GFIT to evaluate potential broadband noise reduction capabilities with and without flow. When either the source SPL or flow Mach number was increased (i.e., SPL $>$ 120 dB, Mach $>$ 0.0), the resistance spectra were above the optimum and the number of resonances decreased from two to one for the variable facesheet liner. As a result, the absorption of this liner became similar to that achieved with uniform liners. In the next investigation, geometries will be optimized based on a targeted frequency range and flow condition.

The Prony method was used to educe the impedance of each GFIT sample, and those impedances, their respective measured inlet and exit sound pressure levels and phases, along with the appropriate flow conditions, were used as inputs to the CHE propagation code to predict the acoustic pressure profiles in the GFIT. This process demonstrated the validity of the computational tools used in the design, as reasonable agreement was seen between the computational and experimental results.

Acknowledgements

The authors would like to thank Brian Howerton and Max Reid for their dedication in acquiring data for this research. This work was funded by the Advanced Air Transport Technology Project of the NASA Advanced Air Vehicles Program.

References

[1]Brown, M. C. and Jones, M. G., "Evaluation of Variable Facesheet Liner Configurations for Broadband Noise Reduction," AIAA Paper 2020-2616, AIAA AVIATION 2020 Forum, Virtual Event, June 2020.

[2]Jones, M. G., Howerton, B. M., and Ayle, E., "Evaluation of Parallel-Element, Variable-Impedance, Broadband Acoustic Liner Concepts," AIAA Paper 2012-2194, 18th AIAA/CEAS Aeroacoustics Conference, Colorado Springs, CO, June 2012.

[3]Jones, M. G., Parrott, T. L., and Watson, W. R., "Uncertainty and Sensitivity Analyses of a Two-Parameter Impedance Prediction Model," AIAA Paper 2008-2928, 14th AIAA/CEAS Aeroacoustics Conference, Vancouver, British Columbia Canada, May 2008.

[4]Jones, M. G., Nark, D. M., and Watson, W. R., "Evaluation of a Multizone Impedance Eduction Method," AIAA Paper 2019-2486, 25th AIAA/CEAS Aeroacoustics Conference, Delft, The Netherlands, May 2019.

[5]Bendat, J. S. and Piersol, A. G., *Random Data: Analysis and Measurement Procedures*, Wiley-Interscience, 1971.

[6]Jones, M. G., Watson, W. R., Howerton, B. M., and Busse-Gerstengarbe, S., "Comparative Study of Impedance Eduction Methods, Part 2: NASA Tests and Methodology," AIAA Paper 2013-2125, 19th AIAA/CEAS Aeroacoustics Conference, Berlin, Germany, May 2013.

[7]Jones, M. G., Watson, W. R., Nark, D. M., Schiller, N. H., and Born, J. C., "Optimization of Variable-Depth Liner Configurations for Increased Broadband Noise Reduction," AIAA Paper 2016-2783, 22nd AIAA/CEAS Aeroacoustics Conference, Lyon, France, May 2016.

[8]Motsinger, R. E. and Kraft, R. E., "Design and Performance of Duct Acoustic Treatment: Aeroacoustics of Flight Vehicles; Chapter 14, Vol. 2: Noise Control," NASA RP 1258, Aug. 1991.